

# Investigation of the $K^-pp$ Bound State via the $K^- + {}^3\text{He}$ Reaction

Sajjad Marri<sup>1,\*</sup> and Ahmad Naderi Beni<sup>2</sup>

<sup>1</sup>*Department of Physics, Isfahan University of Technology, Isfahan 84156-83111, Iran*

<sup>2</sup>*Department of Basic Sciences, Technical and Vocational University (TVU), Tehran, Iran*

Using the four-body Alt-Grassberger-Sandhas (AGS) equations for the  $K^-ppn$  system, we investigate the possible formation of a  $K^-pp$  quasi-bound state through the low-energy  $K^- + {}^3\text{He}$  reaction. The neutron missing mass spectrum in the final state was calculated for different models of the  $\bar{K}N$  interaction. The results indicate that, irrespective of the specific nature of the  $\Lambda(1405)$  structure or the details of the  $\bar{K}N$  interaction model, a signal corresponding to the  $K^-pp$  quasi-bound state could appear in the  $\pi\Sigma p$  mass spectrum. This supports the feasibility of observing the  $K^-pp$  cluster in low-energy kaon-induced reactions on helium-3.

PACS numbers: 13.75.Jz, 14.20.Pt, 21.85.+d, 25.80.Nv

arXiv:2602.19716v1 [nucl-th] 23 Feb 2026

---

\* [marri@iut.ac.ir](mailto:marri@iut.ac.ir)

## I. INTRODUCTION

The interaction between antikaons ( $\bar{K}$ ) and nucleons plays a significant role in the study of strongly interacting kaonic systems. This interaction, characterized by its attractive nature in the isospin-zero channel, has garnered considerable attention due to its connection to exotic nuclear states and its implications for understanding low-energy quantum chromodynamics (QCD) [1–5]. One of the most intriguing manifestations of this interaction is the possible existence of the  $K^-pp$  system, a three-body configuration composed of an antikaon and two protons [6–18]. The study of this system provides insight into the underlying meson-baryon dynamics and the nature of the  $\Lambda(1405)$  resonance, which is dynamically generated by the coupling of  $\bar{K}N$  and  $\pi\Sigma$  channels [1, 2].

The theoretical prediction of deeply bound antikaonic nuclear states was first proposed by Akaishi and Yamazaki [6, 7], who suggested that the strong attraction of the antikaon in the  $I = 0$  channel could lead to the formation of compact, high-density nuclear configurations. Their calculations indicated the existence of a bound  $K^-pp$  state with a binding energy of approximately 48 MeV and a width of about 61 MeV. Subsequent studies employing different theoretical approaches, including Faddeev calculations [8–11], have investigated the  $K^-pp$  system with varying predictions for its binding energy and decay width. Recent coupled-channel three-body studies have shown that explicit particle-channel dynamics can significantly modify the properties of the  $K^-pp$  quasi-bound state [19]. These discrepancies highlight the complexity of the system and the challenges in reliably describing the interplay between the antikaon and the two-nucleon core and the sensitivity of the results to the input interactions.

Experimental efforts to observe the  $K^-pp$  state have included proton-proton collisions, stopped-kaon reactions, and photoproduction experiments. The DISTO experiment at SATURNE reported a structure in  $pp$  collisions suggesting a binding energy of around 103 MeV and a width of about 118 MeV [20]. Similarly, the FINUDA collaboration observed a peak in the  $\Lambda p$  invariant mass spectrum consistent with a binding energy of roughly 115 MeV and a width of 67 MeV [21]. However, these findings remain controversial due to possible final-state interaction effects [22, 23]. In particular, the FINUDA results were later re-examined by the AMADEUS collaboration [24], which concluded that the observed spectrum can be fully explained by  $K^-$  multi-nucleon absorption processes, without requiring a  $K^-pp$  component. The J-PARC E27 experiment, investigating the reaction  $\pi^+ + d$ , also reported a broad structure, though its interpretation was complicated by background processes [25, 26]. The CLAS collaboration at Jefferson Lab studied kaonic clusters through photoproduction, while the AMADEUS experiment at DAΦNE investigated low-energy kaonic systems using low-momentum kaons [27]. Despite these efforts, no conclusive evidence for the  $K^-pp$  state was found. The lack of a distinct signal may indicate a very broad width or the absence of a conventional three-body bound state.

The interaction between an antikaon and a helium-3 nucleus ( $K^- + {}^3\text{He}$ ) provides a promising avenue for probing the  $K^-pp$  state through kaon-induced reactions. The J-PARC E15 experiment utilized such interactions to study the system via neutron missing mass spectroscopy (Fig. 1). Investigating the  $K^- + {}^3\text{He}$  reaction is particularly valuable, as it may help isolate signals of the  $K^-pp$  state while reducing background contributions. Their results suggested a signal corresponding to a bound state with a binding energy of approximately 42 MeV and a decay width of 100 MeV [28, 29]. However, challenges persist: low-momentum kaon beams have low production rates, and low-energy neutrons are difficult to detect due to their weak interaction and low kinetic energy. Consequently, the J-PARC beamline is optimized for a kaon momentum of about 1 GeV/c, balancing production efficiency, detection, and resolution. While low-energy studies may offer theoretical benefits, they remain experimentally demanding.

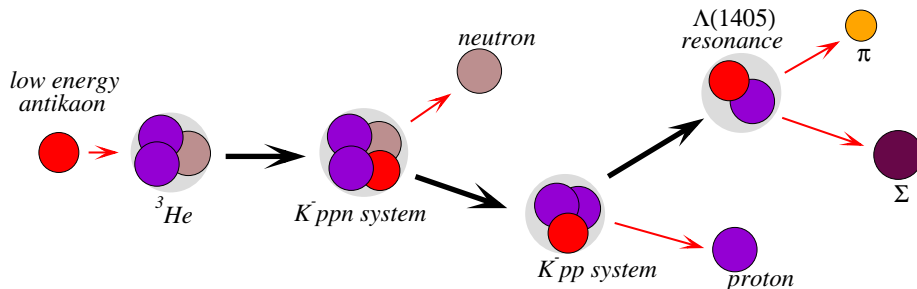


FIG. 1. (Color online) Schematic representation of the transition from  $K^- + {}^3\text{He}$  to  $n + (\pi\Sigma p)$  via the intermediate  $N + (\bar{K}NN)_{s=0}$  state.

Sekihara and collaborators analyzed the  $K^- + {}^3\text{He}$  reaction to interpret the  $\Lambda p$  invariant mass spectrum reported by E15 [30]. They considered scenarios where the incident kaon induces a reaction ejecting a fast neutron, leaving behind a residual two-nucleon system interacting with the antikaon. This intermediate system could either produce a non-resonant  $\Lambda(1405)$ -proton pair or form a quasi-bound  $\bar{K}NN$  state. Their simulations indicated that only the latter could reproduce the observed spectrum, with features attributed to both the decay of the quasi-bound state and kinematical enhancements from quasi-free scattering.

Previous theoretical studies of kaon-induced reactions on light nuclei, in particular the works by Ohnishi *et al.* [31] and Marri *et al.* [32], have investigated the  $\bar{K}NN-\pi\Sigma N$  system using non-relativistic Faddeev calculations. Both works solved the three-body problem to explore the signature of the  $K^-pp$  quasi-bound state. The main distinction lies in the interaction models: Ohnishi *et al.* employed chiral  $\bar{K}N$  potentials [15], whereas Marri *et al.* used phenomenological potentials developed by Shevchenko [33, 34]. Furthermore, Marri *et al.* also observed contributions from the  $\Lambda(1405)$  resonance in addition to the  $\bar{K}^-pp$  signal. In the present work, we extend these studies by performing a four-body calculation of the  $K^- + {}^3\text{He} \rightarrow \pi\Sigma pn$  reaction, which allows us to explicitly study the neutron missing-mass spectrum and provide absolute cross sections, thus offering more direct guidance for experimental investigations.

This study examines the feasibility and advantages of the reaction  $K^- + {}^3\text{He} \rightarrow n + \pi\Sigma p$  as a probe for the  $K^-pp$  bound state. The hypothesized state is expected to decay into multiple final states, including  $\pi\Sigma p$ . Since the  $\pi\Sigma$  subsystem is closely tied to the  $\Lambda(1405)$ , often regarded as a  $\bar{K}N$  quasi-bound state, detecting  $\pi\Sigma$  pairs with a proton offers insight into the decay mechanisms of  $K^-pp$ . Neutron detection enables missing mass reconstruction, providing a powerful tool for isolating signals from competing background processes. High-resolution invariant mass reconstruction of the  $\pi\Sigma p$  system, combined with neutron kinematics, enhances sensitivity to the binding energy and width of the state. The complexity of the multi-particle final state allows for improved discrimination between genuine bound states and final-state interaction effects, increasing the robustness of the experimental conclusions.

In this work, we apply the four-body Faddeev approach to the  $K^- + {}^3\text{He}$  system to calculate the neutron missing mass spectrum and assess the presence of a  $K^-pp$  bound state. Our framework incorporates recent models of the  $\bar{K}N$  interaction and aligns with existing experimental constraints. The results contribute to the ongoing efforts to determine the existence and properties of the  $K^-pp$  system and to enhance our understanding of few-body meson-baryon dynamics.

From an experimental point of view, the present calculations are relevant to a setup in which the outgoing neutron is detected. Using the measured neutron momentum and the known initial-state kinematics, the invariant mass of the  $(\pi\Sigma p)$  subsystem can be reconstructed via the neutron missing-mass technique. Therefore, the quantity discussed throughout this work as the neutron missing-mass spectrum is equivalent to the  $\pi\Sigma p$  invariant-mass distribution. Although a fully exclusive measurement detecting all four final-state particles  $(\pi, \Sigma, p, n)$  is, in principle, possible, the neutron missing-mass method provides a more practical and experimentally feasible approach.

The paper is organized as follows. Section II introduces the formalism for the four-body  $\bar{K}NNN$  system and outlines the transition amplitude for the  $K^- + {}^3\text{He}$  reaction. Section III discusses the two-body inputs and presents the calculated mass spectra. Finally, Sec. IV provides our conclusions.

## II. FORMALISM: FOUR-BODY FADDEEV EQUATIONS

One can investigate the properties of the  $\bar{K}NNN$  system using the Faddeev Alt–Grassberger–Sandhas (AGS) formalism, focusing specifically on the state with total angular momentum  $J = \frac{1}{2}$  and isospin  $I = 0$ . By treating the three nucleons as identical particles and simplifying the analysis by neglecting their intrinsic spin and isospin degrees of freedom, the system can be described in terms of three distinct partitions:

1. Partition  $\sigma = 1$ : A configuration consisting of an antikaon ( $\bar{K}$ ) and a three-nucleon cluster ( $NNN$ ), denoted as  $[\bar{K} + (NNN)]$ .
2. Partition  $\sigma = 2$ : A single nucleon ( $N$ ) coupled with a  $\bar{K}NN$  subsystem, represented as  $[N + (\bar{K}NN)]$ .
3. Partition  $\sigma = 3$ : A system composed of a  $\bar{K}N$  pair and an  $NN$  pair, described as  $[(\bar{K}N) + (NN)]$ .

Before we proceed to present the four-body formalism, by systematically addressing each partition and employing the Faddeev-AGS formalism, we aim to shed light on the intricate interactions within the  $\bar{K}NNN$  system and identify possible quasi-bound states that may emerge from these interactions. In partitions  $\sigma = 1$  and  $\sigma = 2$ , the quasi-particles are three-body systems. To obtain the observables related to these subsystems, one should solve the three-body Faddeev equations. For a system including three particles  $i, j$ , and  $k$ , the three-body Faddeev equations in the AGS form can be expressed as [35]:

$$\mathcal{K}_{ij, I_i I_j}^\sigma = \mathcal{M}_{ij, I_i I_j}^\sigma + \sum_{k, I_k} \mathcal{M}_{ik, I_i I_k}^\sigma \tau_{k I_k}^\sigma \mathcal{K}_{kj, I_k I_j}^\sigma, \quad \sigma = 1, 2 \quad (1)$$

where  $\mathcal{K}_{ij, I_i I_j}^\sigma$  represents the transition operators,  $\mathcal{M}_{ij, I_i I_j}^\sigma$  are the driving terms, and  $\tau_{k I_k}^\sigma$  is an energy-dependent part of a separable two-body  $T$ -matrices within the three-body system. In the Faddeev equations 1, the isospin quantum number of the interacting particle pair  $(j, k)$ , with particle  $i$  as the spectator, is denoted by  $I_i$ . Solving these equations provides insight into the dynamics and possible bound or quasi-bound states of the three-body subsystems, such as  ${}^3\text{He}$ ,  $\bar{K}(NN)_{s=0}$  and  $\bar{K}(NN)_{s=1}$ , which are essential for understanding the structure and reaction dynamics of the full four-body  $\bar{K}NNN$  system.

The Faddeev equations in (1) can give complete description for three-nucleon subsystem. For  $\bar{K}(NN)_{s=0,1}$  since the  $\bar{K}N$  is coupled with  $\pi\Sigma$  channel, one should consider the  $\pi\Sigma N$  channel into the calculations. Therefore, in Faddeev equations (1) plus the Faddeev partition indices  $i, j, k = 1, 2, 3$ , one should modify the Faddeev equations to take the  $\bar{K}N - \pi\Sigma$  coupling directly into account. Thus, in addition to the pair of Faddeev indices, each transition operator or driving term in Eq. (1) should also carry a pair of particle channel indices, of type  $\alpha, \beta, \gamma \dots$ , each one having three possibilities, namely  $\bar{K}N_1N_2, \pi\Sigma N_2$  or  $\pi N_1\Sigma$ . See [9, 10, 36] for details.

In our three- and four-body calculations, the so-called exact optical potential method [33] was employed to simplify the Faddeev equations. This method avoids the complexity of solving the full three- and four-body equations, which are computationally demanding and may suffer from convergence difficulties. It provides a substantial simplification while retaining a high level of accuracy, making it a reliable approximation for treating coupled channels. Consequently, when solving the Faddeev equations (Eq. (1)) for the  $\bar{K}NN - \pi\Sigma N$  system, the  $\pi\Sigma N$  channel was not included explicitly. The unnecessary particle channel indices have been omitted.

Since the total isospin of the  $\bar{K}NN$  system is  $I = 1/2$ , therefore, depending on the spin of the two baryons, we should treat  $K^-pp$  or  $K^-d$  system. The total isospin of the interacting particles determines their total spin quantum number. Consequently, spin indices of the baryons do not appear explicitly, and the operators are labeled solely by isospin indices. In the  $K^-pp$  system the spin component is antisymmetric, so all operators in isospin base should be symmetric and in the case of  $K^-d$ , all operators in isospin base should be antisymmetric.

To solve the three-body equations, it is beneficial to represent the three-body amplitudes and driving terms in a separable form. This approach transforms the equations (1) into a homogeneous form, facilitating their solution. In this work, we employ the EDPE (Energy-Dependent Pole Expansion) method, as detailed in Refs. [37–39]. The separable representation of the Faddeev transition amplitudes is expressed as:

$$\mathcal{K}_{ij, I_i I_j}^\sigma(q, q'; \epsilon_\sigma) = \sum_{\mu, \nu}^{N_r} u_{\mu, i I_i}^\sigma(q, \epsilon_\sigma) \theta_{ij; \mu\nu}^{\sigma; I_i I_j}(\epsilon_\sigma) u_{\nu, j I_j}^\sigma(q', \epsilon_\sigma), \quad (2)$$

where  $u_{\mu, i I_i}^\sigma$  and  $u_{\nu, j I_j}^\sigma$  are the form factors associated with the interacting subsystems, and  $\theta_{ij; \mu\nu}^{\sigma; I_i I_j}(\epsilon_\sigma)$  are the elements of the coupling matrix that encapsulate the interaction dynamics between different partitions. The variables  $q$  and  $q'$  represent the momenta of the spectator particle in channels  $i$  and  $j$  of the three-body subsystem, respectively.

The eigen functions  $u_{\mu, i I_i}^\sigma(q, \epsilon_\sigma)$  in Eq. (2) can be defined by solving the homogeneous Faddeev equations

$$\begin{aligned} u_{\mu, i I_i}^\sigma(q, \epsilon_\sigma) &= \frac{1}{\lambda_\mu^\sigma} \sum_{j I_j} \int \mathcal{M}_{ij, I_i I_j}^\sigma(q, q'; \epsilon_\sigma) \\ &\times \tau_{j I_j}^\sigma(\epsilon_\sigma - \frac{q'^2}{2M_j^\sigma}) u_{\nu, j I_j}^\sigma(q', \epsilon_\sigma) d\vec{q}', \end{aligned} \quad (3)$$

by solving Eq. (3), one can determine the possible binding energy  $B_\sigma$  of the three-body system, along with the corresponding form factors  $u_{\mu, i I_i}^\sigma(q, B_\sigma)$  and eigenvalues  $\lambda_\mu^\sigma$  at the energy  $\epsilon_\sigma = B_\sigma$ . The form factors can be normalized by the condition

$$\begin{aligned} \sum_{i=1}^3 \int u_{\mu, i I_i}^\sigma(q, B_\sigma) \tau_{i I_i}^\sigma(q, B_\sigma) u_{\nu, i I_i}^\sigma(q, B_\sigma) d\vec{q} \\ = -\delta_{\mu\nu}. \end{aligned} \quad (4)$$

In Eq. (3), the form factors are defined at a fixed energy  $\epsilon_\sigma = B_\sigma$ , corresponding to the binding energy of the three-body system. To extend the applicability of the eigenfunctions  $u_{\mu, i I_i}^\sigma$  across the entire energy and momentum spectrum, we perform an extrapolation by

$$\begin{aligned} u_{\mu, i I_i}^\sigma(q, \epsilon_\sigma) &= \frac{1}{\lambda_\mu^\sigma} \sum_{j I_j; \beta} \int \mathcal{M}_{ij, I_i I_j}^\sigma(q, q'; \epsilon_\sigma) \\ &\times \tau_{j I_j}^\sigma(q', B_\sigma) u_{\nu, j I_j}^\sigma(q', B_\sigma) d\vec{q}'. \end{aligned} \quad (5)$$

After determining the eigenfunctions  $u_{\mu, i I_i}^\sigma(q, \epsilon_\sigma)$ , one can define the effective EDPE propagators  $\theta(\epsilon_\sigma)$  in Eq. (2) by

$$\begin{aligned} ((\theta^\sigma(\epsilon_\sigma))^{-1})_{\mu\nu} &= \sum_{i I_i} \int [u_{\mu, i I_i}^\sigma(q, B_\sigma) \tau_{i I_i}^\sigma(q, B_\sigma) \\ &- u_{\mu, i I_i}^\sigma(q, \epsilon_\sigma) \tau_{i I_i}^\sigma(q, \epsilon_\sigma)] u_{\nu, i I_i}^\sigma(q, \epsilon_\sigma) d\vec{q}. \end{aligned} \quad (6)$$

Based on Eq. (6), the Faddeev indices ( $i, j$  and  $k$ ) and isospin indices ( $I_i$  and  $I_j$ ) of the  $\theta^\sigma(\epsilon_\sigma)$ -functions are unnecessary and could be omitted. Therefore, we have

$$\theta_{ij;\mu\nu}^{\sigma;I_i I_j}(\epsilon_\sigma) = \theta_{\mu\nu}^\sigma(\epsilon_\sigma). \quad (7)$$

In addition to solving the three-body subsystems, it is essential to address the Faddeev equations for configurations involving two independent pairs of interacting particles, referred to as two quasi-particles. Specifically, we consider the  $(\bar{K}N)(NN)_{s=0,1}$  subsystem. To analyze this state, we define the corresponding eigenfunctions. The pertinent equations are given by:

$$\begin{aligned} \mathcal{Y}_{ij;I_i I_j}^\sigma &= \mathcal{W}_{ij;I_i I_j}^\sigma + \mathcal{W}_{ij;I_i I_j}^\sigma \tau_{jI_j}^\sigma \mathcal{Y}_{jj;I_j I_j}^\sigma, \\ \mathcal{Y}_{jj;I_j I_j}^\sigma &= \mathcal{W}_{jj;I_j I_j}^\sigma \tau_{iI_i}^\sigma \mathcal{Y}_{ij;I_i I_j}^\sigma, \quad \sigma = 3, \end{aligned} \quad (8)$$

where the operators  $\mathcal{Y}_{ij;I_i I_j}^\sigma$  are the Faddeev amplitudes which describe two independent pairs of interacting particles and the operator  $\mathcal{W}_{ij;I_i I_j}^\sigma$  is the effective potential. In the same way as it was in the [3+1] subsystems, the eigenfunctions  $u_{\mu;iI_i}^\sigma$  can be defined by solving the homogeneous Faddeev equations

$$u_{\mu;iI_i}^\sigma(q, \epsilon_\sigma) = \frac{1}{\lambda_\mu^\sigma} \mathcal{W}_{ij;I_i I_j}^\sigma(q, q'; \epsilon_\sigma) \tau_{jI_j}^\sigma(\epsilon_\sigma) u_{\mu;jI_j}^\sigma(q', \epsilon_\sigma). \quad (9)$$

Now that we have found the solution for the subsystems, we can go to solve the Faddeev equations for  $\bar{K}NNN$  four-body system. Transition amplitudes between all possible partitions of the  $\bar{K}NNN$  are given by [40, 41].

$$\begin{aligned} \mathcal{A}_{\sigma(i)\rho(j)}^{I_i I_j, \mu\nu} &= \mathcal{R}_{\sigma(i)\rho(j)}^{I_i I_j, \mu\nu} + \sum_{\omega;kl;\lambda\kappa} \sum_{I_k, I_l} \mathcal{R}_{\sigma(i)\omega(k)}^{I_i I_k, \mu\lambda} \\ &\quad \times \theta_{kl;\lambda\kappa}^{\omega;I_k I_l} \mathcal{A}_{\omega(l)\rho(j)}^{I_l I_j, \kappa\nu}, \end{aligned} \quad (10)$$

where  $\mathcal{A}_{\sigma(i)\rho(j)}^{I_i I_j, \mu\nu}$  is the Faddeev transition amplitude from  $\rho$  to  $\sigma$  partition. To identify the spectator particle or interacting particles in each two- and three-body subsystem, we utilized the indices  $i, j$  and  $k$ . The indices  $\mu$  and  $\nu$  refer to the separable expansion of the subamplitudes (equation 2). The operators  $\mathcal{R}_{\sigma(i)\rho(j)}^{I_i I_j, \mu\nu}$  represent the driving terms, which describe the effective potential realized by the exchanged particle or quasi-particle between the channels  $\sigma$  and  $\rho$

$$\begin{aligned} \mathcal{R}_{\sigma(i)\rho(j)}^{I_i I_j, \mu\nu}(p, p', E) &= \frac{\Omega_{\sigma(i)\rho(j)}^{I_i I_j}}{2} \int_{-1}^{+1} d(\hat{p} \cdot \hat{p}') \\ &\quad \times u_{\mu,iI_i}^\sigma(q, \epsilon_\sigma) \tau_{iI_i}^\sigma(p, p'; z) u_{\nu,jI_j}^\rho(q', \epsilon_\rho). \end{aligned} \quad (11)$$

The symbols  $\Omega_{\sigma(i)\rho(j)}^{I_i I_j}$  denote the Clebsch–Gordan coefficients. For a detailed explanation of the parameters in Eq. (11), the reader is referred to Refs. [40, 42]. The functions  $u_{\mu,iI_i}^\sigma$  are the form factors that arise in the separable representation of the sub-amplitudes, as defined in Eqs. (3) and (9).

Looking for a scattering amplitude needs solution of the inhomogeneous system of equations (10), which can be written in a matrix form

$$\mathcal{A} = \mathcal{R} + \mathcal{K}\mathcal{A}, \quad (12)$$

where the operator  $\mathcal{K}$  is the kernel of the four-body Faddeev equations. The four-body scattering amplitude can be defined by

$$\mathcal{A} = (I - \mathcal{K})^{-1} \mathcal{R}. \quad (13)$$

In this work, we focus on the  $K^- + {}^3\text{He}$  reaction as a potential avenue for observing the  $K^- pp$  bound state. We analyze one specific reaction channel:



In this scenario, the intermediate state consists of a neutron and a  $\bar{K}NN$  three-body system with total spin  $s = 0$ . By analyzing the neutron missing mass spectrum in this specific reaction channel, we aim to identify a potential signal corresponding to the formation of the  $K^- pp$  bound state. A distinct peak in the missing mass spectrum would provide evidence supporting the existence of this deeply bound state.

The transition from the initial  $K^- + {}^3\text{He}$  state to the final  $n + \pi\Sigma p$  channel involves a series of intricate processes, as illustrated in Figure 1. Initially, the system undergoes a transformation from  $K^- + {}^3\text{He}$  to an intermediate state characterized

by  $N + (\bar{K}NN)_{s=0}$ . This stage represents a complex four-body interaction, encompassing an antikaon ( $K^-$ ) and a helium-3 nucleus ( ${}^3\text{He}$ ). To accurately determine the transition amplitude for this process, it is essential to solve the inhomogeneous four-body Faddeev equations (10).

Subsequently, the intermediate  $(\bar{K}NN)_{s=0}$  system, in the presence of a spectator nucleon ( $N$ ), decays into the  $\pi\Sigma N$  channel. This decay process is influenced by the isospin state ( $I = 0$  and  $I = 1$ ) of the  $(\bar{K}N)$  system, which dictates the possible decay pathways and the resulting particle configurations. In summary, the transition from  $K^- + {}^3\text{He}$  to  $n + \pi\Sigma p$  encompasses a sequence of complex interactions, including the formation of an intermediate four-body state and its subsequent decay. Employing the Faddeev formalism provides a robust framework for analyzing these processes, offering valuable insights into the underlying physics of few-body systems and the interactions governing them. Therefore, the scattering amplitude ( $\mathcal{T}$ ) for the  $K^- + {}^3\text{He} \rightarrow n + (\pi\Sigma p)$  reaction channel can be defined by [43]

$$\begin{aligned} \mathcal{T} = & \sum_{I_{NN}=0,1} \sum_{I_{\bar{K}N}=0,1} \sum_{\lambda,\mu,\nu=1}^{N_r} \mathcal{A}_{1(N)2(N)}^{I_{NN}I_{\bar{K}N},\mu\lambda}(P_{K^-}, p_n; E) \\ & \times \theta_{\lambda\nu}^{\rho=2}(p_n, E) u_{\nu,pI_p}^{\rho=2}(p_n, q_p; E) \\ & \times \tau_{\bar{K}N \rightarrow \pi\Sigma}^{I=0,1}(p_n, q_p; E) g_{\pi\Sigma}^{I=0,1}(p_n, q_p; E), \end{aligned} \quad (14)$$

where  $p_n$  denotes the momentum of the spectator neutron,  $q_p$  represents the spectator proton momentum in the  $K^- pp$  three-body subsystem when the proton acts as the spectator particle. In Eq. 14, the functions  $u_{\nu,iI_i}^\rho$  and  $\theta_{\lambda\nu}^\rho$  were obtained by solving the one-channel Faddeev AGS equations. The total cross section in center of mass coordinates can be calculated by

$$\begin{aligned} \sigma = & (4\pi)^3 \int p_n^2 dp_n \int q_p^2 dq_p \int k_{\pi\Sigma}^2 dk_{\pi\Sigma} \delta(E_f - E_i) \\ & \times \frac{(2\pi)^4}{|\vec{v}_{K^-} - \vec{v}_{{}^3\text{He}}|} |\mathcal{T}|^2, \end{aligned} \quad (15)$$

where  $\mathcal{T}$  is the scattering amplitude calculated in Eq. 14 and the energies  $E_i$  and  $E_f$  are given by

$$\begin{aligned} E_i = & \frac{P_{K^-}^2}{2m_{K^-}} + \frac{P_{K^-}^2}{2m_{{}^3\text{He}}} + \Delta mc^2 - B_{{}^3\text{He}} \\ E_f = & \frac{k_{\pi\Sigma}^2}{2\mu_{\pi\Sigma}} + \frac{p_n^2(m_n + m_p + m_\pi + m_\Sigma)}{2m_n(m_p + m_\pi + m_\Sigma)} \\ & + \frac{q_p^2(m_p + m_\pi + m_\Sigma)}{2m_p(m_\pi + m_\Sigma)}. \end{aligned} \quad (16)$$

The  $\delta$ -function can be written in terms of  $k_{\pi\Sigma}$  in the form

$$\delta(E_f - E_i) = \left| \frac{1}{\frac{dE_f}{dk_{\pi\Sigma}} \Big|_{k_{\pi\Sigma}=k_{\pi\Sigma}^0}} \right| \delta(k_{\pi\Sigma} - k_{\pi\Sigma}^0), \quad (17)$$

where the momentum  $k_{\pi\Sigma}^0$  is defined by

$$\begin{aligned} k_{\pi\Sigma}^0 = & \sqrt{2\mu_{\pi\Sigma}} \left[ E_i - \frac{p_n^2(m_n + m_p + m_\pi + m_\Sigma)}{2m_n(m_p + m_\pi + m_\Sigma)} \right. \\ & \left. - \frac{q_p^2(m_p + m_\pi + m_\Sigma)}{2m_p(m_\pi + m_\Sigma)} \right]^{1/2}. \end{aligned} \quad (18)$$

Therefore, the neutron missing mass can be written in the form

$$\begin{aligned} d\sigma/dE_n = & (4\pi)^3 \int q_p^2 dq_p \frac{(2\pi)^4 m_{K^-} m_{{}^3\text{He}}}{P_{K^-} (m_{K^-} + m_{{}^3\text{He}})} \\ & \times k_{\pi\Sigma}^0 \mu_{\pi\Sigma} p_n |\mathcal{T}|^2, \end{aligned} \quad (19)$$

TABLE I. Model dependence of the  $\bar{K}N$  and  $\bar{K}(NN)_{s=0}$  pole positions (in MeV). Results are presented for the phenomenological SIDD1 and SIDD2 potentials, as well as the chiral-based  $\bar{K}N-\pi\Sigma$  interaction. The SIDD1 model yields a single-pole structure, whereas the SIDD2 and chiral-based potentials reproduce the two-pole structure of the  $\Lambda(1405)$  resonance.

	SIDD1	SIDD2	Chiral
$\bar{K}N$ first pole	1428.1 - i46.6 [34]	1418.1 - i56.9 [34]	1420.6 - i20.3 [15]
$\bar{K}N$ second pole	—	1382.0 - i104.2 [34]	1343.0 - i72.5 [15]
$K^-pp$ pole position	2325 - i34	2325 - i24	2346 - i22

where  $E_n$  denote the energy of the outgoing neutron.

Although the differential cross section is formally calculated as a function of the neutron energy,  $d\sigma/dE_n$ , the results are presented in terms of the invariant mass of the  $\pi\Sigma p$  subsystem. This choice reflects the experimental relevance of the  $\pi\Sigma p$  invariant-mass spectrum and its direct connection to the  $K^-pp$  and  $\Lambda(1405)$  signals.

The two variables are related through energy conservation in the center-of-mass frame. For a fixed initial energy  $E_{\text{tot}}$ , the invariant mass of the  $\pi\Sigma p$  system is given by

$$\begin{aligned} M_{\pi\Sigma p} &= m_\pi + m_\Sigma + m_p + (E_i - E_n) \\ &= m_\pi + m_\Sigma + m_p + \left(E_i - \frac{p_n^2}{2m_n}\right). \end{aligned} \quad (20)$$

Thus, the neutron missing-mass spectrum and the  $\pi\Sigma p$  invariant-mass spectrum represent equivalent descriptions of the same physical observable, related by a change of kinematical variables. In the present work, we use  $M_{\pi\Sigma p}$  as the horizontal axis in the figures for clarity.

### III. RESULTS AND DISCUSSIONS

In this paper, we consider all two-body interactions to have zero orbital angular momentum. The primary interactions examined are between antikaon-nucleon ( $\bar{K}N$ ) and nucleon-nucleon ( $NN$ ) pairs. The  $\bar{K}N$  subsystem predominantly couples with the pion-Sigma ( $\pi\Sigma$ ) channel in isospin states  $I = 0$  and with  $\pi\Sigma$  and  $\pi\Lambda$  channels in  $I = 1$ . For the  $\bar{K}N$  interaction, we utilize separable potential in the momentum representation, defined as:

$$V_I^{\alpha\beta}(k^\alpha, k^\beta) = g_I^\alpha(k^\alpha) \lambda_I^{\alpha\beta} g_I^\beta(k^\beta), \quad (21)$$

where  $g_I^\alpha(k^\alpha)$  is the form factor of the interacting two-body subsystem, with relative momentum  $k^\alpha$  and isospin  $I$  and  $\lambda_I^{\alpha\beta}$  is the strength parameter of the interaction. To take the  $\bar{K}N - \pi\Sigma$  coupling directly into account, the potential is further labeled with the  $\alpha$  values. The two-body  $T$ -matrices in separable form can be given by

$$T_I^{\alpha\beta}(k^\alpha, k^\beta; z) = g_I^\alpha(k^\alpha) \tau_I^{\alpha\beta}(z) g_I^\beta(k^\beta), \quad (22)$$

where  $z$  is the total energy of the two-body subsystem and the quantity  $\tau_{i,i}^{\alpha\beta}(z)$  is an energy-dependent part of a separable two-body  $T$ -matrix.

To describe the coupled-channel  $\bar{K}N-\pi\Sigma$  interaction, which plays a crucial role in both our three- and four-body calculations, we employ two different phenomenological potentials and one chiral potential. These potentials are constructed to reproduce either a one-pole or a two-pole structure of the  $\Lambda(1405)$  resonance. The parameters of the phenomenological potentials, denoted as SIDD1 and SIDD2, are taken from Ref. [34], while those of the energy-dependent chiral potential are given in Ref. [15]. The corresponding pole positions for each potential model are summarized in Table I. In addition to the  $\bar{K}N$  pole position, we have also calculated the  $K^-pp$  pole position using the one-channel AGS equations.

For modeling nucleon-nucleon ( $NN$ ) interaction, we utilize the one-term PEST potential [44]. This potential serves as a separable approximation to the Paris potential, focusing primarily on the attractive long-range component of the  $NN$  interaction while omitting the short-range repulsive part. Consequently, this simplification leads to an overestimation of the binding energy in light nuclei, such as helium-3 ( $B_{\text{He}} = 10.7$  MeV).

Since the kernel of AGS equations has the standard moving singularities that are caused by the opened channels and are encountered in any three and four-body breakup problem, we have followed the same procedure implemented in Refs. [45, 46].

In few-body scattering calculations, particularly those employing the Faddeev or Alt–Grassberger–Sandhas (AGS) formalism, the kernel integrals often contain singular terms of the form

$$\frac{1}{E - E_p + i\varepsilon}, \quad (23)$$

which become problematic when the total energy  $E$  approaches the pole position  $E_p$ . Direct numerical integration in this region is unstable due to the divergence induced by the vanishing denominator. To handle this issue, the *point method* is frequently applied [45, 46].

The core idea of the point method is to avoid evaluating the integral exactly at the singular energy. Instead, one computes the scattering amplitude (or any required quantity) at several nearby complex energies

$$E_j = E + i\varepsilon_j, \quad \varepsilon_j > 0, \quad (24)$$

where  $\varepsilon_j$  are small positive shifts that move the integration contour off the real axis. At each shifted energy  $E_j$ , the integrals are well-defined and can be evaluated numerically without encountering divergences:

$$X(E_j) = \int_0^\infty \frac{f(p)}{E_j - p^2} dp. \quad (25)$$

Once the values  $X(E_j)$  have been obtained for several  $\varepsilon_j$ , one assumes analyticity of  $X(E)$  in the vicinity of the real axis and performs an analytic continuation:

$$X(E) = \lim_{\varepsilon \rightarrow 0^+} X(E + i\varepsilon). \quad (26)$$

In practice, this continuation is achieved by fitting  $X(E_j)$  as a function of  $\varepsilon_j$  using either a polynomial expansion or a Padé approximant. This approach avoids the need for explicit principal-value integration or complex contour deformation, while maintaining numerical stability. It is particularly advantageous for above-threshold energies, where singularities are unavoidable and computational efficiency is essential.

Using the transition amplitude defined in Eq. (14), the missing mass of the spectator nucleon ( $d\sigma/dE_n$ ) was calculated. As a first step, the four-body transition amplitude in Eq. (14) was turned off by setting  $\mathcal{A}_{\sigma(i)\rho(j)}^{I_i I_j, \mu \lambda} = 1$ , and the neutron missing mass spectrum was computed. In this case, only the interactions within the dashed ellipse in Fig. 2 were included. The corresponding results are shown in Fig. 3.

The incoming antikaon momentum was set to  $p_{K^-} = 100 \text{ MeV}/c$ , and the missing mass of the neutron was evaluated using three different  $\bar{K}N$  interaction models. In these calculations, the number of terms  $N_r$  in Eq. (2) was fixed to  $N_r = 2$ , which ensures sufficient numerical accuracy for practical purposes.

A pronounced peak associated with the  $K^-pp$  bound state appears for all interaction models. However, compared to the values reported in Table I, the peak position is shifted by approximately 10-15 MeV toward the  $\pi\Sigma p$  threshold, regardless of the chosen  $\bar{K}N$  potential. Additionally, a structure related to the  $\Lambda(1405)$  resonance emerges in the spectra obtained with the chiral-based and SIDD2 potentials. This feature appears as a shoulder on the main  $K^-pp$  peak. In contrast, for the SIDD1 potential, the  $\Lambda(1405)$  signal is strongly affected by threshold effects, since the  $\Lambda(1405) + p$  mass threshold lies very close to  $M(^3\text{He}) + m(K^-) - M(n)$ .

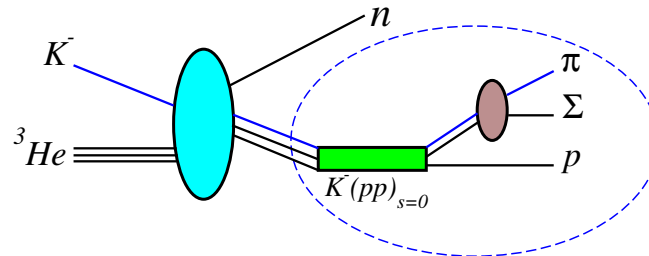


FIG. 2. (Color online) Schematic representation of the transition from  $K^- + ^3\text{He}$  to  $n + (\pi\Sigma p)$  via the intermediate state  $N + (\bar{K}NN)_{s=0}$ . The large solid ellipse denotes the four-body dynamics of the initial system, while the rectangular box represents the three-body dynamics associated with the formation and decay of the  $\bar{K}NN$  cluster.

Theoretical studies using Faddeev calculations have indicated that the formation of a bound  $K^-pp$  state could manifest as a distinct peak in the  $\pi\Sigma N$  invariant mass [31, 32]. It was also shown in [32] that the  $\Lambda(1405)$  resonance manifests itself in the  $\pi\Sigma N$  mass spectrum. However, these calculations were three-body type approximations of the  $K^- + ^3\text{He}$  interaction and the

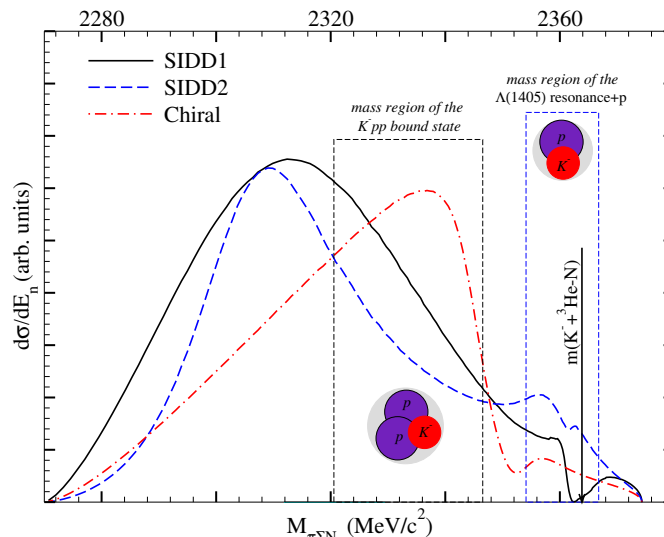


FIG. 3. (Color online) The neutron missing mass spectrum is presented. In this analysis, the full four-body Faddeev amplitude is not included; instead, only the reaction mechanisms within the region within the dashed ellipse in Fig. 2 are considered. A clear peak associated with the  $K^-pp$  bound state is visible for all interaction models examined. In addition to the  $K^-pp$  signal, an enhancement attributed to the  $\Lambda(1405)$  resonance appears in the spectrum, particularly when using the SIDD2 and chiral potentials. In contrast, for the SIDD1 potential, the  $\Lambda(1405)$  pole lies above the threshold, which is reflected in the corresponding spectral distribution.

full dynamics of the four-body system and the effect of the spectator neutron were not included properly. The results presented in Fig. 2 are in good agreement with those reported in Ref. [32], where it was shown that, in addition to the  $K^-pp$  bound state signal, the signature of the  $\Lambda(1405)$  resonance appears in the  $\pi\Sigma p$  invariant mass spectrum.

In Fig. 4, we performed a full four-body calculation of the reaction  $K^- + ^3\text{He} \rightarrow (\pi\Sigma p) + n$  to analyze the spectral features in the final-state channels. Our approach incorporates the full dynamics of the antikaon interacting with the three-nucleon system, accounting for all relevant couplings and decay mechanisms leading to the  $(\pi\Sigma p) + n$  final state. The computed spectrum reveals a clear enhancement near the  $\bar{K}NN$  pole position threshold in the invariant mass distribution of the  $\pi\Sigma p$ . The characteristics of the calculated spectrum particularly the peak location below the  $K^-pp$  threshold and its moderate width are not reproduced by non-resonant or purely kinematical mechanisms. This structure is consistent in both peak position and width with the pole energies reported in Table I. This indicates that the observed enhancement is a genuine manifestation of strong  $\bar{K}N$  attraction in the isospin-zero channel, leading to a tightly bound few-body configuration. The results are qualitatively consistent with the enhancement observed by the E15 experiment and interpreted by Sekihara *et al.* as a  $K^-pp$ -like state. However, at the lower kaon momentum used in our study, the peak is sharper and less distorted by background, supporting the hypothesis that low-energy  $K^-$  beams are better suited for studying such quasi-bound states. This enhancement is attributed to the reduced momentum transfer and the resulting increased overlap between the kaon and the  $^3\text{He}$  system, facilitating the formation of a quasi-bound  $\bar{K}NN$  configuration. Further exclusive measurements of the  $(\pi\Sigma p)$  spectrum, including angular correlations, will be valuable for constraining the binding energy and decay width of this exotic system and for advancing our understanding of antikaon-nuclear interactions.

A comparison of the  $\pi\Sigma p$  mass spectra obtained using the chiral-based potential (red dashed and dotted curve) and the SIDD2 potential (blue dashed curve) with those calculated within the three-body approximation (Fig. 2) shows that a similar peak structure associated with the  $K^-pp$  bound state is observed in both cases. However, the peak corresponding to the  $\Lambda(1405)$  resonance does not clearly appear in the spectrum extracted from the four-body calculation, which is possibly due to the effects of four-body dynamics.

A clear difference is observed when comparing the three-body results in Fig. 3 with the full four-body calculations shown in Fig. 4, most notably for the SIDD1 interaction. While the three-body dynamics exhibits a pronounced signal of the  $K^-pp$  quasi-bound state together with the  $\Lambda(1405)$  resonance, the inclusion of the spectator neutron and full four-body kinematics leads to a strong suppression of the  $K^-pp$  signal and an enhancement of the  $\pi\Sigma$  strength. This behavior can be attributed to the single-pole structure and stronger subthreshold attraction of the SIDD1  $\bar{K}N$  potential. In the four-body framework, recoil effects and additional off-shell dynamics redistribute the spectral strength toward the  $\pi\Sigma$  channel, thereby favoring the  $\Lambda(1405)$  contribution. In contrast, for the SIDD2 and chiral interactions, which exhibit a two-pole structure of the  $\Lambda(1405)$ , the transition from three- to four-body dynamics results in only moderate changes of the mass spectrum.

Recently, Shevchenko [19] performed a coupled-channel three-body calculation including additional particle channels, leading to a less bound and broader  $K^-pp$  quasi-bound state. A fully coupled-channel four-body treatment would be considerably more complex and is beyond the scope of the present work. Nevertheless, these results indicate that explicit particle-channel effects

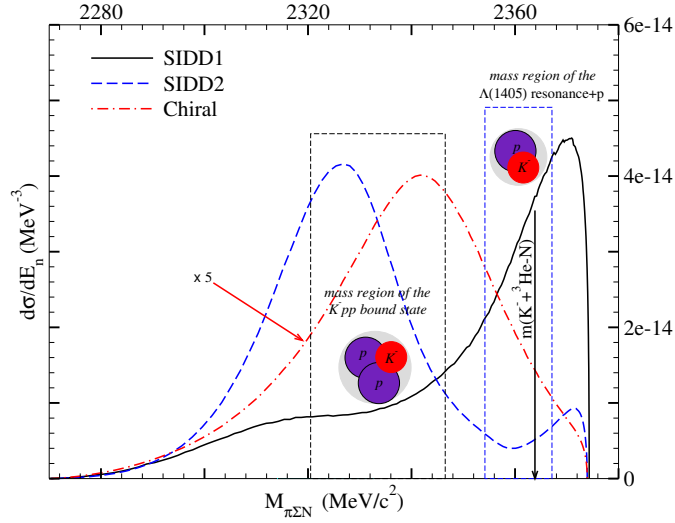


FIG. 4. Calculated neutron missing mass spectrum for the  $K^- + {}^3\text{He} \rightarrow n + (\pi\Sigma p)$  reaction at a kaon momentum of 100 MeV/c. The explanations are the same as in Fig. 3. Here, the full four-body Faddeev calculations was performed to determine the neutron mass spectrum.

may further modify the properties of the  $K^-pp$  system.

In this work, we present theoretical calculations of the reaction  $K^- + {}^3\text{He} \rightarrow n + (\pi\Sigma p)$ , focusing on a low kaon momentum of 100 MeV/c. The choice of a low-energy kaon is motivated by several advantages: near-threshold quasi-bound states, such as  $K^-pp$ , are more prominently formed and can be studied with greater clarity, while the reduced kinetic energy limits the phase space for background processes, making signals from the desired channels more distinct. Additionally, at lower energies, theoretical modeling becomes more controlled, as fewer reaction channels are open, allowing for a more precise treatment of the dynamics using few-body techniques. The low-momentum regime also aligns with the validity of the  $\bar{K}N$  interaction models employed in this work (SIDD1, SIDD2, and Chiral potentials), which are effective primarily in the low-energy region. Moreover, our framework enables the calculation of the neutron missing-mass spectrum and absolute cross sections, providing direct guidance for experimental searches of the  $K^-pp$  quasi-bound state. Although the J-PARC E15 experiment [29] employs a higher kaon momentum of about 1 GeV/c, the essential reaction mechanisms, including the formation of the  $K^-pp$  quasi-bound state and contributions from the  $\Lambda(1405)$  resonance, are qualitatively comparable. Hence, our results provide complementary insights into the reaction dynamics and serve as guidance for the interpretation of spectral shapes observed in E15 and future low-momentum kaon experiments.

#### IV. CONCLUSION

In conclusion, our four-body calculation of the  $K^- + {}^3\text{He} \rightarrow (\pi\Sigma p) + n$  reaction at an incoming kaon momentum of 100 MeV/c demonstrates that low-energy kaons are highly effective in probing  $\bar{K}NN$  dynamics. The results show enhanced signal strength between the  $\pi\Sigma N$  and  $\bar{K}NN$  thresholds, supporting the interpretation of a  $\bar{K}NN$  bound state. In comparison with E15 data and the theoretical framework of Sekihara *et al.*, our findings suggest that low-momentum kaon beams offer significant advantages for identifying and studying such exotic states. Moreover, the comparison of different  $\bar{K}N$  interaction models indicates that the spectral features are sensitive to the underlying coupled-channel dynamics, emphasizing the importance of a consistent treatment of the  $\Lambda(1405)$  in few-body calculations. Our model, which fully accounts for the four-body nature of the initial system, offers a refined description compared to simpler few-body approaches. It accurately represents the nuclear environment and final-state dynamics, reinforcing the interpretation of the E15 signal as evidence for a  $\bar{K}NN$  bound state. Our findings suggest that future experiments optimized for low-energy kaon beams and improved neutron detection could provide clearer evidence for the existence and properties of  $K^-pp$ -like systems. The theoretical predictions made in this study pave the way for such investigations and contribute to the ongoing effort to understand the strong interaction in the strangeness sector.

- 
- [1] N. Kaiser, P. B. Siegel, and W. Weise, Nucl. Phys. A **594**, 325 (1995).  
 [2] E. Oset and A. Ramos, Nucl. Phys. A **635**, 99 (1998).  
 [3] J. A. Oller and U. G. Meissner, Phys. Lett. B **500**, 263 (2001).

- [4] D. Jido *et al.*, Nucl. Phys. A **725**, 181 (2003).
- [5] Y. Kamiya *et al.*, Nucl. Phys. A **954**, 41 (2016).
- [6] Y. Akaishi and T. Yamazaki, Phys. Rev. C **65**, 044005 (2002).
- [7] T. Yamazaki and Y. Akaishi, Phys. Lett. B **535**, 70 (2002).
- [8] N. V. Shevchenko, A. Gal, and J. Mares, Phys. Rev. Lett. **98**, 082301 (2007).
- [9] N. V. Shevchenko *et al.*, Phys. Rev. C **76**, 044004 (2007).
- [10] Y. Ikeda and T. Sato, Phys. Rev. C **76**, 035203 (2007).
- [11] Y. Ikeda and T. Sato, Phys. Rev. C **79**, 035201 (2009).
- [12] A. Dote, T. Hyodo, and W. Weise, Nucl. Phys. A **804**, 197 (2008).
- [13] A. Dote, T. Hyodo, and W. Weise, Phys. Rev. C **79**, 014003 (2009).
- [14] S. Wycech and A. M. Green, Phys. Rev. C **79**, 014001 (2009).
- [15] Y. Ikeda, H. Kamano, and T. Sato, Prog. Theor. Phys. **124**, 533 (2010).
- [16] M. Bayar, J. Yamagata-Sekihara, and E. Oset, Phys. Rev. C **84**, 015209 (2011).
- [17] N. Barnea, A. Gal, and E. Z. Liverts, Phys. Lett. B **712**, 132 (2012).
- [18] A. Dote, T. Inoue, and T. Myo, Prog. Theor. Exp. Phys. **2015**, 043D02 (2015).
- [19] N. V. Shevchenko, Phys. Rev. C **112**, 064007 (2025).
- [20] T. Yamazaki *et al.*, Phys. Rev. Lett. **104**, 132502 (2010).
- [21] M. Agnello *et al.*, Phys. Rev. Lett. **94**, 212303 (2005).
- [22] A. Dote *et al.*, Prog. Theor. Phys. Suppl. **146**, 508 (2002).
- [23] V. K. Magas *et al.*, Phys. Rev. C **74**, 025206 (2006).
- [24] R. Del Grande *et al.*, (AMADEUS Collaboration), Eur. Phys. J. C **79**, 190 (2019).
- [25] Y. Ichikawa *et al.*, Few-Body Syst. **54**, 1191 (2013).
- [26] Y. Ichikawa *et al.*, Prog. Theor. Exp. Phys. **2015**, 021D01 (2015).
- [27] O. Vázquez Doce (AMADEUS Collaboration), Hyperfine Interact. **193**, 195 (2009).
- [28] T. Yamaga *et al.* (J-PARC E15 Collaboration), Phys. Rev. C **102**, 044002 (2020).
- [29] T. Yamaga *et al.* (J-PARC E15 Collaboration), Phys. Rev. C **110**, 014002 (2024).
- [30] T. Sekihara, E. Oset, and A. Ramos, Prog. Theor. Exp. Phys. **2016**, 123D03 (2016).
- [31] S. Ohnishi *et al.*, Phys. Rev. C **88**, 025204 (2013).
- [32] S. Marri, S. Z. Kalantari, and J. Esmaili, Chin. Phys. C **43**, 064102 (2019).
- [33] N. V. Shevchenko, Phys. Rev. C, **85**, 034001 (2012).
- [34] N. V. Shevchenko, Nucl. Phys. A **890–891**, 50 (2012).
- [35] E. O. Alt, P. Grassberger, and W. Sandhas, Phys. Rev. C **1**, 85 (1970).
- [36] J. Revai, Few-Body Syst., **54**, 1865 (2013)
- [37] I. M. Nardodetsky, Nucl. Phys. A **221**, 191 (1974).
- [38] S. Nakaichi *et al.*, Phys. Rev. A **26**, 1 (1982).
- [39] A. Fix and H. Arenhövel, Phys. Rev. C **68**, 044002 (2003).
- [40] S. Marri and J. Esmaili, Eur. Phys. J. A **55**, 43 (2019).
- [41] N. V. Shevchenko, Phys. Rev. C **106**, 064006 (2022).
- [42] S. Marri and S. Z. Kalantari, Eur. Phys. J. A **52**, 282 (2016).
- [43] V. F. Kharchenko, V. E. Kuzmichev and S. A. Shadchin, Nucl. Phys. A **226**, 71-92 (1974).
- [44] H. Zankel, W. Plessas, and J. Haidenbauer, Phys. Rev. C **28**, 538 (1983).
- [45] L. Schlessinger, Phys. Rev. **167**, 1411 (1968).
- [46] H. Kamada, Y. Koike, and W. Glöckle, Prog. Theor. Phys. **109**, 869 (2003).